Journal of Applied Fluid Mechanics, Vol. 8, No. 4, pp. 871-883, 200x.
Available online at www.jafmonline.net, ISSN 1735-3572, EISSN 1735-3645.
DOI: 10.18869/acadpub.jafm.67.223.23336

Mathematical Analysis of Single and Two-Phase Flow of Blood in Narrow Arteries with Multiple Contrictions

D. S. Sankar[1†], A. K. Nagar[2] and A. V. Kumar[3]

[1] *Engineering Mathematics Unit, Faculty of Engineering, Institut Teknologi Brunei, Jalan Tungku Link, Gadong BE1410, Brunei Darussalam*
[2] *Department of Mathematics and Computer Science, Centre for Applicable Mathematics and Systems Science, Liverpool Hope University, Hope Park, Liverpool L16 9JD, UK*
[3] *Department of Mathematics, National Institute of Technology, Yupia- 791112, Arunachal Pradesh, India*

†*Corresponding Author Email: sankar_ds@yyahoo.co.in*

(Received June 10, 2014; accepted August 19, 2014)

ABSTRACT

The pulsatile flow of blood in narrow arteries with multiple-stenoses under body acceleration is analyzed mathematically, treating blood as (i) single-phase Herschel-Bulkley fluid model and (ii) two-phase Herschel-Bulkley fluid model. The expressions for various flow quantities obtained by Sankar and Ismail (2010) for single-phase Herschel-Bulkley fluid model and Sankar (2010c) for two-phase Herschel-Bulkley fluid model are used to compute the data for comparing these fluid models in a new flow geometry. It is noted that the plug core radius, wall shear stress and longitudinal impedance to flow are marginally lower for two-phase H-B fluid model than those of the single-phase H-B fluid model. It is found that the velocity decreases significantly with the increase yield stress of the fluid and the reverse behavior is noticed for longitudinal impedance to flow. It is also noticed that the velocity distribution and flow rate are higher for two-phase Herschel-Bulkley fluid model than those of the single-phase Herschel-Bulkley fluid model. It is also recorded that the estimates of the mean velocity increase with the increase of the body acceleration and this behavior is reversed when the stenosis depth increases.

Keywords: Blood flow; Single-phase fluid flow; Two-phase fluid flow; Body acceleration; Multiple-stenoses; Comparative study.

NOMENCLATURE

B	body acceleration parameter
e	pressure gradient parameter
n	power law index
p	dimensionless pressure
Q	dimensionless flow rate
$R(z)$	dimensionless radius of the artery in the stenosed region
α	pulsatile Reynolds number ratio
α_H	pulsatile Reynolds number of Herschel-Bulkley fluid
α_N	pulsatile Reynolds number of Newtonian fluid
δ_1	semi-depth of the maximum projection of the first stenosis in the single-phase Herschel-Bulkley fluid model
δ_2	semi-depth of the maximum projection of the second stenosis in the single-phase Herschel-Bulkley fluid model
δ_{1P}	semi-depth of the maximum projection of the first stenosis in the peripheral layer region of the two-phase Herschel-Bulkley fluid model
δ_{2P}	semi-depth of the maximum projection of the second stenosis in the peripheral layer region of the two-phase Herschel-Bulkley fluid model
δ_{1C}	semi-depth of the maximum projection of the first stenosis in the core region of the two-phase Herschel-Bulkley fluid model
δ_{2C}	semi-depth of the maximum projection of the second stenosis in the core region of the two-phase Herschel-Bulkley fluid model

Subscripts

H	Herschel
N	Newtonian fluid (used for u, τ)
R_P	dimensionless plug core radius
r	dimensionless radial distance
u_H	dimensionless axial velocity of Herschel-Bulkley fluid
u_N	dimensionless axial velocity of Newtonian fluid
t	dimensionless time
z	dimensionless axial distance

ϕ	lead angle
$\dot{\gamma}$	shear rate
Λ	dimensionless longitudinal impedance to flow
ω	angular frequency of the blood flow
θ	yield stress
ψ	azimuthal angle
τ_H	dimensionless shear stress of Herschel-Bulkley fluid
τ_N	dimensionless shear stress of Newtonian fluid
τ_w	dimensionless wall shear stress
P	plug core region
w	wall shear stress (used for τ)

1. INTRODUCTION

In several circumstances of our routine life, like during our travel in a bus, train, car, aircraft, ship, even while accepting vibration therapy as a treatment process to cardiovascular diseases, we are subjected to body accelerations or vibrations (Chakravarty and Mandal, 1996). In some situations like travelling in a bus/train etc, our whole body is exposed to vibrations, whereas in some other situations like, while operating jack hammer or lathe machine, specific part of our body is subjected to accelerations (Nagarani and Sarojamma, 2008; El-Shehawey et al., 2000). The continuous exposure of high level unintended external body accelerations to our body causes disturbance in the blood circulation (El-Shahed, 2003) and this leads to serious diseases which may show the symptoms like frequent headache, abdominal pain, increase in pulse rate, venous pooling of blood in the extremities, hemorrhage in face, neck and eye-sockets, loss of vision etc (Mustapha et al., 2008; Chaturani and Issac, 1995; Usha and Prema, 1999). Hence, the investigation on the blood flow in arteries under periodic body acceleration is important in the diagnosis and therapeutic treatment of health problems (Mandal et al., 2007; Mishra, 1999; Sarojamma and Nagarani, 2002).

Many cardiovascular diseases are known to be responsible for deaths of thousands of people yearly and the origin of most of them are closely related to the nature of blood circulation and the dynamic behavior of the blood vessel (Ang and Mazumdar, 1995). Medical survey reveals that more than 80% of the total deaths of humans are due to the diseases of blood vessel walls (Liepsch, 2002; Rogers, 2011). Among them, arthrosclerosis is a very dangerous disease that is caused due to deposition of cholesterol and some other substances on the endothelium and by the proliferation of connective tissues in the arterial wall (Liepsch et al., 1992). Once a mild stenosis is developed in the lumen of the artery, it causes circulatory disorder in the arteries (Tu and Deville, 1996).

Several researchers studied the blood flow characteristics in the presence of stenoses in the lumen of the arteries (Ikbal et al., 2009; Sankar, 2010a; Ismail et al., 2008). Blood behaves like a Newtonian fluid when it flows in larger diameter arteries at high shear rates. Many studies were carried out to analyze the steady and unsteady flow of blood in larger diameter arteries, treating it as Newtonian fluid (Liu et al., 2004; Chakravarty and Mandal, 2004; Sud and Sekhon, 1985). Blood exhibits remarkable non-Newtonian character when it flows through narrow diameter arteries at low shear rates and blood flow in narrow arteries is highly pulsatile, particularly in diseased state. Several attempts made to study the pulsatile flow of blood through stenosed narrow arteries, modeling it as a non–Newtonian fluid (Chaturani and Palanisamy, 1990; Siddiqui et al., 1999).

Chakravarty et al. (2004) and Mishra et al. (2002) mentioned that when blood flows through narrow blood vessels, there is a peripheral layer of plasma and a core layer with the suspension of all the erythrocytes. Thus, for a realistic description of blood flow in narrow arteries at low shear rates, it is appropriate to model blood as a two-phase fluid model with the suspension of all the erythrocytes in the core region as non-Newtonian fluid and the plasma in the peripheral layer region as Newtonian fluid. Several researchers have studied the two-phase fluid models for blood flow through stenosed arteries treating the fluid in the core region as a non-Newtonian fluid and the plasma in the peripheral layer region as Newtonian fluid (Srivastava and Saxena, 1994; Sankar, 2010b).

Herschel-Bulkley (H- B) fluid is a non-Newtonian fluid model with yield stress which is generally used to model blood when it flows through narrow arteries (Chaturani and Ponnalagar Samy, 1985). Sankar and Ismail (2010) studied the pulsatile flow of single-phase H-B fluid model for blood flow in narrow arteries with single axi-symmetric stenosis under the influence of body acceleration. Sankar (2010c) mathematically analyzed the blood flow with single stenosis in narrow arteries under the influence of body acceleration, treating blood as two-phase H-B fluid model. The pulsatile flow of single-phase and two-phase H-B fluid models for blood flow in a narrow artery with multiple-stenoses under periodic body acceleration was investigated by anyone so far, to the knowledge of the authors. Hence, in the present study, a theoretical study is taken up to compare the pulsatile flow of single-phase H-B fluid model and two-phase H-B fluid model for blood flow in a narrow artery with mild multiple-stenoses under the influence of external periodic body acceleration. In the first model, H-B fluid model is used to represent blood in the entire flow region, whereas in the second model, blood is treated as two-phase fluid flow model with the suspension of all the erythrocytes in the core region is modeled by H-B fluid and the cell-free plasma in the peripheral layer region is represented by Newtonian fluid. The asymptotic solution obtained for the flow quantities by Sankar and Ismail (2010) for single-phase H-B fluid model and Sankar (2010c) for two-phase H-B

fluid model are used to compute the data in new flow geometry (multiple-stenoses) to perform a comparative study among these fluid models. The advantageous of using two-phase H-B fluid model rather than single-phase H-B fluid model for blood flow modeling in a narrow artery are also spelt out. The layout of the paper is as follows.

Section 2 formulates both the fluid model's governing differential equations and boundary conditions and solves them to obtain asymptotic solution to the physiologically important flow quantities such as plug core radius, velocity distribution, flow rate, wall shear stress and longitudinal impedance to flow. The effects of various physical parameters on these flow quantities are analyzed and the flow quantities of different fluid models are compared in section 3. Some possible physiological applications to the present study are also given in section 3. The main findings of the study are summarized in the concluding section 4.

2. MATHEMATICAL FORMULATION

Consider an axially symmetric, laminar, pulsatile and fully developed unidirectional flow of blood (assumed to be viscous incompressible fluid) under the influence of periodic body acceleration through a circular artery with an axially symmetric mild multiple stenoses, blood is modeled as two nonlinear fluid models such as (i) single-phase H-B fluid model and (ii) two-phase H-B fluid model. In the single-phase H-B fluid model, blood is modeled as H-B fluid model in the entire flow region, whereas, in the two-phase H-B fluid model of blood, the suspension of all erythrocytes in the core region is treated as H-B fluid and the cell-free plasma in the peripheral layer region is assumed as Newtonian fluid. Due to the presence of the stenosis in the lumen of the artery wall, it is appropriate to treat the wall of the artery as rigid.

The artery is assumed to be too long so that the entrance and end effects can be neglected. The geometries of the segment of artery with mild multiple stenoses for single-fluid flow and two-fluid flow of blood are shown in Fig.1. Cylindrical polar coordinates system $(\bar{r},\bar{\psi},\bar{z})$ is used to analyze the flow.

Since the size of the stenoses in the lumen of the artery is mild and the flow is assumed to be slow in a narrow artery, the radial component of velocity is negligibly small and can be neglected for low Reynolds number flow. The non-dimensional form of the momentum equation governing the flow is given below (One can refer Sankar and Ismail (2010) for dimensional form of the governing equations).

$$\alpha_H^2 \frac{\partial u_H}{\partial t} = 4\left(1 + e\cos t\right) + 4B\cos\left(\omega t + \phi\right) - \frac{2}{r}\frac{\partial}{\partial r}\left(r\tau_H\right),\ 0 \le r \le R(z) \tag{1}$$

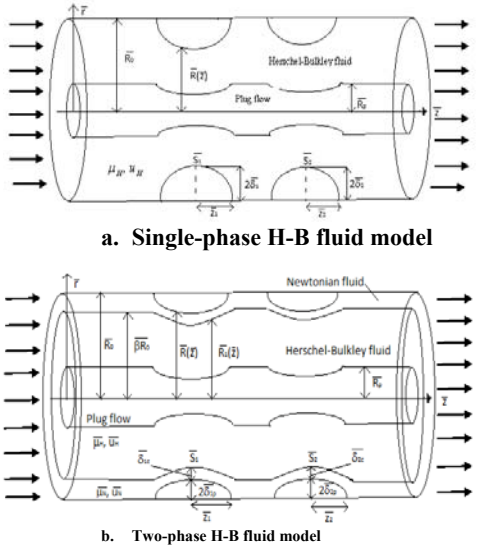

a. Single-phase H-B fluid model

b. Two-phase H-B fluid model

Fig. 1. Geometry of segment of the narrow artery with multiple stenoses.

2.1 Single-Phase H-B Fluid Model

2.1.1 Governing Equations

where α_H pulsatile Reynolds number or Womersley number of H-B fluid model which is mathematically defined as $\alpha_H = \sqrt{\bar{R}_0^{\,2}\bar{\omega}\bar{\rho}/\bar{\mu}_0}$, (where $\bar{\mu}_0 = \bar{\mu}_H\left[2/\bar{R}_0\,\bar{A}_0\right]^{n-1}$, $\bar{A}_0, \bar{R}_0, \bar{\omega}, \bar{\rho}\,\bar{\mu}_0$ and $\bar{\mu}_H$ are the constant pressure gradient of the flow, radius of the normal artery, angular frequency of the flow, blood density, viscosity coefficient having the dimension as that of Newtonian fluid and coefficient of viscosity of H-B fluid respectively (in dimensional form)), τ_H , u_H are the shear stress and axial component of the velocity; e and B are the parameters for the pressure gradient and body acceleration respectively; t, ω and ϕ are the parameters for time, angular frequency and phase angle of the flow respectively, R is the radius of the artery. The non-dimensional form of the constitutive equation of the H-B fluid which models blood is

$$\frac{\partial u_H}{\partial r} = \begin{cases} -2\left(\tau_H - \theta\right)^n & \text{if } \tau_H \ge \theta \text{ and } R_P \le r \le R \\ 0 & \text{if } \tau_H \le \theta \text{ and } 0 \le r \le R_P \end{cases} \tag{2}$$

where θ is the non-dimensional form of the yield stress and R_P is the plug core radius. Eq. (2) signifies that normal shear flow happens in the regions where the shear stress exceeds the yield stress and plug flow (or solid like flow) occurs in the regions where the shear stress does not exceed the yield stress. The boundary conditions in the non-dimensional form are

$$\tau_H \text{ is finite at } r = 0 \tag{3}$$

$$u_H = 0 \text{ at } r = R(z) \tag{4}$$

The geometry of segment of an artery with multiple stenoses in dimensionless form is mathematically defined by

$$R(z)=\begin{cases} a_1(t)\left[1-\delta_1\left(1+\cos z'\right)\right], & \text{if } S_1' \le z \le S_1'' \\ a_1(t)\left[1-\delta_2\left(1+\cos z''\right)\right], & \text{if } S_2' \le z \le S_2'' \\ a_1(t) & \text{otherwise} \end{cases} \tag{5}$$

where $z'=\pi(z-S_1)/Z_1$; $z''=\pi(z-S_2)/Z_2$; $S_1'=S_1-Z_1$; $S_1''=S_1+Z_1$; $S_2'=S_2-Z_2$; $S_2''=S_2+Z_2$; δ_1, δ_2 are the maximum heights of first and second stenosis respectively such that $\delta_1/R_0 << 1$, S_1-Z_1, S_2-Z_2 and S_1+Z_1, S_2+Z_2 are the start and end positions of the first and second stenosis, $a_1(t)$ represents the time dependent changes in the radius of the artery. The non-dimensional volume flow rate $Q(t)$ is given by

$$Q(z,t)=4\int_0^{R(z)} u(z,r,t)\; r\; dr \tag{6}$$

2.1.2 Method of Solution

Since Eqs. (1) and (2) form a system of nonlinear partial differential equations, it is not possible to obtain an exact solution to this system of differential equations. Hence, perturbation method with pulsatile Reynolds number α_H as the small parameter of the series expansion is employed to solve this system of nonlinear partial differential equations. Since the present study deals with pulsatile flow of blood and the square of the pulsatile Reynolds number (α_H^2) occurs naturally in the non-dimensionalize form of the momentum equation and is very small, it is more appropriate to expand the unknowns u_H and τ_H (appearing in Eqs. (1) and (2)) in the perturbation series about α_H^2. Let us expand the velocity u_H in the perturbation series about the square of the pulsatile Reynolds number α_H^2 (where $\alpha_H^2 << 1$) as shown below.

$$u_H(r,z,t)=u_{H0}(r,z,t)+\alpha_H^2 u_{H1}(r,z,t)+\ldots \tag{7}$$

Similarly, the shear stress $\tau_H(r,z,t)$, the plug core radius $R_p(z,t)$, the plug core velocity $u_p(z,t)$, and the plug core shear stress $\tau_p(z,t)$ can be expanded in perturbation series about α_H^2. Applying the perturbation series expansions of u_H and τ_H in Eq. (1) and then equating the constant terms and α_H^2 terms, one can get

$$\frac{\partial}{\partial r}(r\tau_{H0})=2r\left[(1+e\cos t)+B\cos(\omega t+\phi)\right], \tag{8}$$

$$\frac{\partial u_{H0}}{\partial t}=-\frac{2}{r}\frac{\partial}{\partial r}(r\tau_{H1}). \tag{9}$$

Using the binomial series approximation in Eq. (2) and then using the perturbation series expansions of u_H and τ_H in the resulting equation and then equating the constant terms and α_H^2 terms, one can obtain

$$-\frac{\partial u_{H0}}{\partial r}=2\tau_{H0}^{n-1}\left[\tau_{H0}-n\theta\right], \tag{10}$$

$$-\frac{\partial u_{H1}}{\partial r}=2n\,\tau_{H0}^{n-2}\;\tau_{H1}\left[\tau_{H0}-(n-1)\theta\right]. \tag{11}$$

Applying the perturbation series expansions of u_P and τ_P in the boundary conditions (3) and (4), one can get

τ_{P0} and τ_{P1} are finite at $r=0$, (12)

$u_{H0}=0$ and $u_{H1}=0$ at $r=0$. (13)

Integrating Eq. (8) between 0 and R_{P0}, then using the condition that τ_{P0} is finite at $r=0$, we obtain

$$\tau_{P0}=g(t)R_{P0} \tag{14}$$

where $g(t)=(1+e\cos t)+B\cos(\omega\tau+\phi)$. Integrating Eq. (8) between R_{P0} and r and using Eq. (14), we get

$$\tau_{H0}=g(t)r. \tag{15}$$

Using Eq. (15) into Eq. (10) and then integrating it between r and $R(=R(z))$ with the help of first of the boundary condition (13), we obtain

$$u_{H0}=2\left[g(t)R\right]^n R \times\left[\left(1/(n+1)\right)\left\{1-(r/R)^{n+1}\right\}-\left(q^2/R\right)\left\{1-(r/R)^n\right\}\right] \tag{16}$$

where $q^2=(\theta/g(t))$. The plug core velocity u_{0p} can be obtained from Eq. (16) as

$$u_{P0}=2\left[g(t)R\right]^n R \times\left[\left(1/(n+1)\right)\left\{1-(R_{0P}/R)^{n+1}\right\}-\left(q^2/R\right)\left\{1-(R_{0P}/R)^n\right\}\right]. \tag{17}$$

Neglecting the terms involving α_H^2 and higher powers of α_H in the perturbation series expansion of R_p and using Eq. (14), the expression for R_{P0} can be obtained as

$$r|_{\tau_{P0}=\theta}=R_{P0}=\theta/g(t)=q^2. \tag{18}$$

Using Eq. (18) in Eq. (17), one can obtain

$$u_{P0}=2\left[g(t)R\right]^n R \times\left[\left(1/(n+1)\right)\left\{1-\left(q^2/R\right)^{n+1}\right\}-\left(q^2/R\right)\left\{1-\left(q^2/R\right)^n\right\}\right] \tag{19}$$

Similarly, solving Eqs. (9) and (11) with the boundary conditions (12) and (13) and Eqs. (14) – (19), the expressions for τ_{P1}, τ_{H1}, u_{H1} and u_{P1} can be obtained as given in Appendix A.One can obtain the expression for the correction in the velocity distribution u_{P1} can be obtained from Eq. (A3) by replacing r by $q^2\left(=R_{P0}^2\right)$. The wall shear stress τ_{HW} is a physiologically important quantity which plays an important role in determining aggregate sites of platelets (Chaturani and Ponnalagar Samy,

1985). The expression for wall shear stress τ_{HW} is given by

$$\tau_{HW} = \left(\tau_{H0} + \alpha_H^2\, \tau_{H1}\right)_{r=R} = \left[g(t)\, R\right] \times\left[1-\left(\left(g(t)R\right)^{n-1} \alpha_H^2 R^2 D \Big/ \left(2(n+2)(n+3)\right)\right) \times\left\{n(n+2)-(n-1)n(n+3)\left(q^2/R\right)-3\left(n^2+2n-2\right)\left(q^2/R\right)^{n+3}\right\}\right] \tag{20}$$

From Eq. (6) and the expressions for velocity, the expression for the volumetric flow rate $Q(z,t)$ is obtained as in Appendix B. The correction to the plug core radius R_{1P} can be obtained by neglecting the terms with α_{H}^4 and higher powers of α_H in the perturbation series expansion of R_{P} in the following manner. The shear stress $\tau_H = \tau_{H0} + \alpha_H^2\, \tau_{H1}$ at $r = R_{\mathrm{P}}$ is given by

$$\left[\tau_{H0} + \alpha_H^2\, \tau_{H1}\right]_{r=R_P} = \theta. \tag{21}$$

From the Taylor's series expansion of τ_{H0} and τ_{H1} about R_{P0} and $\tau_{H0}\big|_{r=R_{P0}} = \theta$, we get

$$R_{P1} = \left(-\tau_{H1}\big|_{r=R_{P0}}\right) \Big/ g(t). \tag{22}$$

Using Eqs. (21) and (22) in the perturbation series expansion of R_P, we obtain

$$R_P = q^2 + \alpha_H^2 \left[g(t)R\right]^{n-1}\left(nDR^3/2(n+1)\right) \times\left[\left(q^2/R\right)-\left(\left(n^2-1\right)/n\right)\left(q^2/R\right)^2 -\left(q^2/R\right)^{n+2}\right] \tag{23}$$

The longitudinal impedance (or resistive impedance) to flow in the artery is defined by

$$\Lambda = g(t)/Q(z,t). \tag{24}$$

2.2 Two-Phase H-B Fluid Model

2.2.1 Governing Equations

For low Reynolds number slow flow of blood (viscous incompressible fluid) in a narrow artery with mild axially symmetric multiple stenoses, the radial component of the velocity is negligibly small and can be neglected. Blood is modeled as two-phase fluid model with the suspension of all the erythrocytes in the core region is represented by H-B model and the cell free plasma in the peripheral layer region is treated Newtonian fluid. The non-dimensional form of the basic momentum equations governing the flow in the core and peripheral layer regions are given below respectively (One shall refer Sankar (2001c) for the dimensional form of the governing equations).

$$\alpha_H^2 \frac{\partial u_H}{\partial t} = 4\left(1+e\cos t\right)+4B\cos\left(\omega t+\phi\right) -\frac{2}{r}\frac{\partial}{\partial r}\left(r\tau_H\right) \quad \text{if} \quad 0 \le r \le R_1(z) \tag{25}$$

$$\alpha_N^2 \frac{\partial u_N}{\partial t} = 4\left(1+e\cos t\right)+4B\cos\left(\omega t+\phi\right) -\frac{2}{r}\frac{\partial}{\partial r}\left(r\tau_N\right) \quad \text{if} \quad R_1(z) \le r \le R(z) \tag{26}$$

where α_N is the pulsatile Reynolds number or Womersley number of Newtonian fluid model in the peripheral layer region which is mathematically defined as $\alpha_N = \sqrt{\bar{R}_0^{\,2}\bar{\omega}\bar{\rho}/\bar{\mu}_N}$, (where, $\bar{A}_0, \bar{R}_0, \bar{\omega}, \bar{\rho}$ and $\bar{\mu}_N$ are the constant pressure gradient of the flow, radius of the normal artery, angular frequency of the flow, blood density and coefficient of viscosity of Newtonian fluid model respectively (in dimensional form)); u_H, u_N are the axial component of the fluid's velocity in the core and peripheral layer regions; τ_H, τ_N are the shear stress of the fluid in the core region and peripheral layer region; α_H, e, B, t, ω and ϕ are already defined in section 2.1.1. R and R_1 are the radius of the artery with the peripheral layer region and core region respectively. The non-dimensional form of the constitutive equation of the fluids in the core and peripheral layer region are

$$\frac{\partial u_H}{\partial r} = \begin{cases} -2\left(\tau_H-\theta\right)^n & \text{if } \tau_H \ge \theta \text{ and } R_P(z) \le r \le R_1(z) \\ 0 & \text{if } \tau_H \le \theta \text{ and } 0 \le r \le R_P(z) \end{cases} \tag{27}$$

$$\frac{\partial u_N}{\partial r} = -2\,\tau_N, \quad \text{if} \quad R_1(z) \le r \le R(z) \tag{28}$$

where R_P is the plug core radius. The boundary conditions can be written in their non-dimensional form are

$$\tau_H \text{ is finite at } r = 0 \tag{29}$$

$$\partial u_H/\partial r = 0 \quad \text{at} \quad r = 0 \tag{30}$$

$$\tau_H = \tau_N \quad \text{at} \quad r = R_1(z) \tag{31}$$

$$u_H = u_N \quad \text{at} \quad r = R_1(z) \tag{32}$$

$$u_N = 0 \quad \text{at} \quad r = R(z). \tag{33}$$

The non-dimensional form of the expressions representing the geometry of the stenoses in peripheral layer region and core region are given below.

$$R(z) = \begin{cases} a_1(t)\left[1-\delta_{1P}\left(1+\cos z'\right)\right], & \text{if } S_1' \le z \le S_1'' \\ a_1(t)\left[1-\delta_{2P}\left(1+\cos z''\right)\right], & \text{if } S_2' \le z \le S_2'' \\ a_1(t) & \text{otherwise} \end{cases} \tag{34}$$

$$R_1(z) = \begin{cases} a_1(t)\left[\beta-\delta_{1C}\left(1+\cos z'\right)\right] & \text{, if } S_1' \le z \le S_1'' \\ a_1(t)\left[\beta-\delta_{2C}\left(1+\cos z''\right)\right] & \text{, if } S_2' \le z \le S_2'' \\ a_1(t) & \text{otherwise} \end{cases} \tag{35}$$

where δ_{1P}, δ_{2P} are the maximum height of the first and second stenosis in the peripheral layer region such that $\delta_{1P}/R_0 << 1$, $\delta_{2P}/R_0 << 1$; δ_{1C}, δ_{2C} are the maximum height of the first and second stenosis in the core region such that $\delta_{1C}/R_0 << 1$, $\delta_{2C}/R_0 << 1$; β is the ratio of the central core radius to the radius of the normal artery, z', z'', S_1', S_1'', S_2', S_2'' are defined

in section 2.1.1; $a_1(t)$ represents the time dependent changes in the radius of the artery. The non-dimensional volume flow rate $Q(t)$ is given by

$$Q(z,t) = 4 \int_0^{R(z)} u(z,r,t)\, r\, dr \tag{36}$$

2.2 Method of Solution

Perturbation method is used to solve the system of partial differential equations (25) – (28) with the boundary conditions (29) - (33). Let us expand the plug core velocity u_P and the velocity in the core region u_H in the perturbation series about α_H^2 (where $\alpha_H^2 << 1$) as shown below.

$$u_P(z,t) = u_{P0}(z,t) + \alpha_H^2 u_{P1}(z,t) + \ldots \tag{37}$$

$$u_H(r,z,t) = u_{H0}(r,z,t) + \alpha_H^2 u_{H1}(r,z,t) + \ldots \tag{38}$$

Similarly, one can expand the other unknown quantities τ_P, τ_H, u_N and τ_N in the perturbation series about α_H^2 and α_N^2. Substituting the perturbation series expansions of u_H and τ_H in Eq. (25) and then equating the constant terms and α_H^2 terms, we get

$$\frac{\partial}{\partial r}(r\tau_{H0}) = 2r\left[(1 + e\sin t) + B\cos(\omega t + \phi)\right], \tag{39}$$

$$\frac{\partial u_{H0}}{\partial t} = -\frac{2}{r}\frac{\partial}{\partial r}(r\tau_{H1}). \tag{40}$$

Using the binomial series approximation in Eq. (27) and applying the perturbation series expansions of u_H and τ_H in the resulting equation and then equating the constant terms and α_H^2 terms, one can obtain

$$-\frac{\partial u_{H0}}{\partial r} = 2\tau_{H0}^{n-1}\left[\tau_{H0} - n\theta\right], \tag{41}$$

$$-\frac{\partial u_{H1}}{\partial r} = 2n\tau_{H0}^{n-2}\tau_{H1}\left[\tau_{H0} - (n-1)\theta\right]. \tag{42}$$

Using the perturbation series expansions of u_N and τ_N in Eq. (26) and then equating the constant terms and α_N^2 terms, one can obtain

$$\frac{\partial}{\partial r}(r\tau_{N0}) = 2r\left[(1 + e\sin t) + B\cos(\omega t + \phi)\right], \tag{43}$$

$$\frac{\partial u_{N0}}{\partial t} = -\frac{2}{r}\frac{\partial}{\partial r}(r\tau_{N1}). \tag{44}$$

On substituting the perturbation series expansion of u_N and τ_N in Eq. (28) and then equating the constant terms and α_N^2 terms, we get

$$-\frac{\partial u_{N0}}{\partial r} = 2\tau_{N0} \tag{45}$$

$$-\frac{\partial u_{N1}}{\partial r} = 2\tau_{N1} \tag{46}$$

Applying the perturbation series expansions of u_H, τ_H, u_N and τ_N in Eqs. (29) - (33) and then equating the constant terms and α_H^2 and α_N^2 terms, the boundary conditions reduce respectively to

τ_{0P} and τ_{1P} are finite at $r = 0$ (47)

$\partial u_{0P}/\partial r = 0$ and $\partial u_{1P}/\partial r = 0$ at $r = 0$ (48)

$\tau_{0H} = \tau_{0N}$ and $\tau_{1H} = \tau_{1N}$ at $r = R_1(z)$ (49)

$u_{0H} = u_{0N}$ and $u_{1H} = u_{1N}$ at $r = R_1(z)$ (50)

$u_{0N} = 0$ *and* $u_{1N} = 0$ *at* $r = R(z)$ (51)

Eqs (39) - (46) form a system of partial differential equations which can be solved for the unknowns $u_{0H}, u_{1H}, \tau_{0H}, \tau_{1H}, u_{0N}, u_{1N}, \tau_{0N}$ and τ_{1N} with the help of boundary conditions (47) - (51) and the expressions obtained for these quantities are given in Appendix C. The expression for correction in the plug flow velocity u_{P1} can be obtained from Eq. (33) by evaluating it at $r = R_{P0} = q^2$. The expression for wall shear stress τ_w is obtained by evaluating τ_N at $r = R$ as given below.

$$\begin{aligned}\tau_w &= (\tau_{N0} + \alpha_N^2 \tau_{N1})_{r=R} = \tau_{w0} + \alpha_N^2 \tau_{w1} \\ &= [g(t)R] + \alpha_N^2 \left\{-[g(t)R]DR^2\left[1 - (R_1/R)^4\right]/8\right\} \\ &\quad + \alpha_N^2 \left\{-\left([g(t)R_1]^n/(2(n+2)(n+3))\right)BR_1^2(R_1/R)\right\} \\ &\quad \left[n(n+2) - n(n-1)(n+3)\left(q^2/R_1\right) - 3(n^2+2n-2)\left(q^2/R_1\right)^{n+3}\right]\end{aligned} \tag{52}$$

Using the expression obtained for velocity distribution in Eq. (36), the expression for the volumetric flow rate $Q(z,t)$ can be obtained as in Appendix D. The two term approximated perturbation series expansion of R_P yields the expression for plug core radius as

$$\begin{aligned}R_P &= q^2 + \left(D\alpha_H^2 R^2/4\right)[g(t)R]\left(q^2/R\right)\left\{1 - (R_1/R)^2\right\} \\ &\quad + \left(nD\alpha_H^2 R_1^2/2(n+1)\right)[g(t)R_1]^n \\ &\quad \times\left\{\left(q^2/R_1\right) - \left((n^2-1)/n\right)\left(q^2/R_1\right)^2 - \left(q^2/R_1\right)^{n+2}\right\}\end{aligned} \tag{53}$$

The longitudinal impedance to flow in the artery is defined as

$$\Lambda = g(t)/Q(z,t). \tag{54}$$

3. RESULTS AND DISCUSSION

The main objective of the present mathematical analysis is to compare the physiologically important flow quantities of single-phase H-B fluid model and two-phase H-B fluid model which are used to model the blood when it flows through a narrow artery with multiple mild stenoses at low shear rates under the influence of periodic body acceleration and to spell out the advantageous of using two-phase H-B fluid model rather than single-phase H-B fluid model for blood flow modeling. Also, it is aimed to investigate the effects of various physiological parameters such as maximum depth of the stenoses, pressure gradient, body acceleration, pulsatile Reynolds number, time, angular frequency and lead angle on the flow

measurements such as plug core radius, velocity distribution, flow rate, wall shear stress and longitudinal impedance to flow. To analyze the aforesaid flow quantities and to validate the present study with the published results of others, we use the following range of parameters (Sankar and Ismail, 2010; Sankar, 2010c).

Power law index n: 0.95 - 1.05; Yield stress θ: 0 – 0.2; Pressure gradient e: 0.5 - 0.7; Body acceleration parameter B: 0 – 2; Interface location parameter β: 0.95 – 1; Maximum projection of first stenosiss δ_{1P} ($=\delta_1$ in single-phase H-B fluid model) and second stenosis δ_{2P} ($=\delta_2$ in two-phase H-B fluid model) in the peripheral layer region: 0.05 – 0.15; Maximum projection of first stenosiss $\delta_{1C}=\beta\delta_{1P}$ and second stenosis $\delta_{2C}=\beta\delta_{2P}$ in the core region; Length of segment of the artery: 60.6; Pulsatile Reynolds number α_H: 0.2 – 0.7; Pulsatile Reynolds number ratio $\alpha(=\alpha_N/\alpha_H)$ takes the same value that is given to α_H; α_N is calculated from $\alpha_N=\alpha\alpha_H$ (Sankar, 2010b).

3.1 Plug Core Radius

The variation of plug core radius with axial distance of single-phase H-B fluid model and two-phase H-B fluid model for different values of α,ϕ and e with n = 0.95, t = 296.47°, θ = 0.1, ω = 1, δ_1 = 0.15, δ_2 = 0.1 and B = 1 are shown in Fig. 2a and 2b respectively. One can easily note that all the distribution curves appear to follow the outline of the two stenoses where the plug core radius decreases from the beginning of the constriction (z = 9.376, z = 32.9) until the peak of the stenoses (z = 18.85, z = 41.45) and then it increases until the offset of the constrictions (z = 28.325, z = 50) are reached. At non-stenotic region, plug core radius remain at maximum value. It is seen that when the pulsatile Reynolds number α increases, the plug core radius increases considerably and it decreases significantly with the increase of the pressure gradient and lead angle ϕ. It is also clear that for a given set of values of the parameters, the plug core radius of the two-phase H-B fluid model is marginally higher than that of single-phase H-B fluid model.

3.2 Plug flow Velocity

The axial variation of plug flow velocity of single-phase and two-phase H-B fluid models for different values of the parameters θ, ϕ, δ_{1P} and δ_{2P} with n = 0.95, ω = 1, t = 296.47°, e = 0.5, α = 0.2 and B = 1 are exhibited in Figs. 3a and 3b respectively. It is noted that plug flow velocity of the fluid decreases significantly when it moves from non-stenotic region to stenotic region and attains its minimum value at the mid-point of the stenoses (z = 18.85, z = 41.45) where the depth of the stenoses are maximum and from there, the plug flow velocity increases significantly until it reaches the non-stenotic region. It is also observed that for fixed value of ϕ and increasing values of the yield stress θ and the maximum depth of the stenoses δ_{1P} and δ_{2P}, the plug flow velocity decreases marginally, but it increases marginally with the increase of the lead (phase) angle ϕ while all the other parameters were treated as invariants. It is of important to note that the plug flow velocity of two-fluid H-B model is considerably higher than that of the single-fluid H-B fluid model.

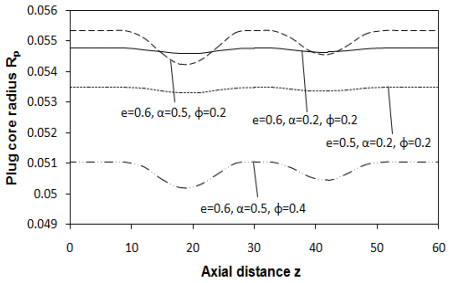

a. Single-phase H-B fluid model.

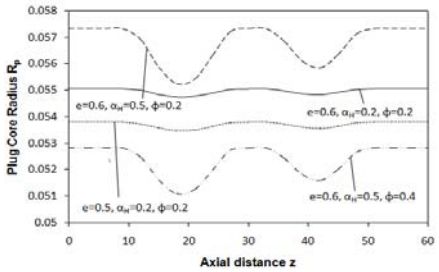

b. Two-phase H-B fluid model with β = 0.95.

Fig. 2. Variation of plug core radius with axial distance for different *e*, α_H and ϕ with n = 0.95, t = 296.47°, θ = 0.1, α = 0.2 , ω = 1 , δ_{1P} = 0.15 , δ_{2P} = 0.1, B = 1.

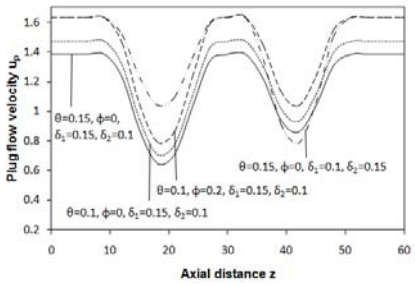

a. Single-phase H-B fluid model.

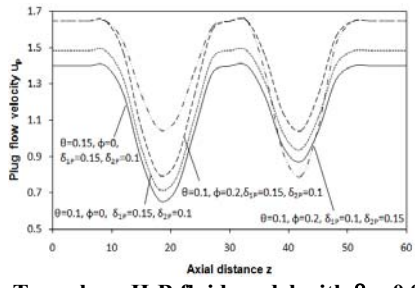

b. Two-phase H-B fluid model with β = 0.95.

Fig. 3. Variation of plug flow velocity with axial distance for different values of θ, ϕ, δ_{1P} and δ_{2P} with n = 0.95, t = 296.47°, e = 0.5, α_H = 0.2, ω = 1, B = 1 and β = 0.95.

3.3 Velocity Distribution

Velocity profiles of single-phase and two-phase H-B fluid models for different values of *B, n,* δ_{1P} and θ with z = 18.85, δ_{2P}, $\alpha_H = \phi = 0.2$, $\omega = 1$ are depicted in Figs. 4a and 4b respectively. One can notice the flattened velocity distribution around the axis of the tube for both of the fluid models. It is clear that the velocity of both of the fluid models increases significantly with the increase of the body acceleration and it decreases considerably when the power law index n increases while all the other parameters were kept as constant. For fixed values of B and n and increasing values of θ and δ_{1P}, the velocity decreases marginally. It is also observed that the velocity distribution of two-phase H-B fluid model is marginally higher than that of single-phase H-B fluid model. It is of important to mention that the plot of the velocity profile in Fig. 8a for single-phase H-B fluid model is in good agreement with the corresponding plot in Fig. 6 of Sankar and Ismail (2010) and the plot of the velocity profile in Fig. 8b for two-phase H-B fluid model is in good agreement with the corresponding plot in Fig. 7 of Sankar (2010).

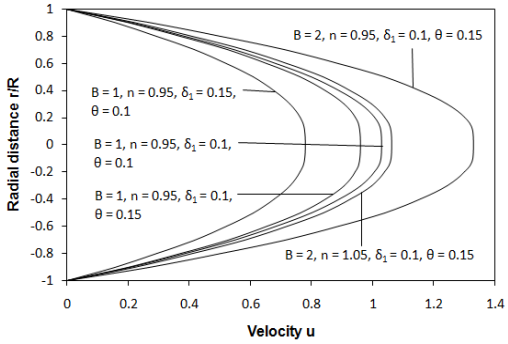

a. Single-phase H-B fluid model.

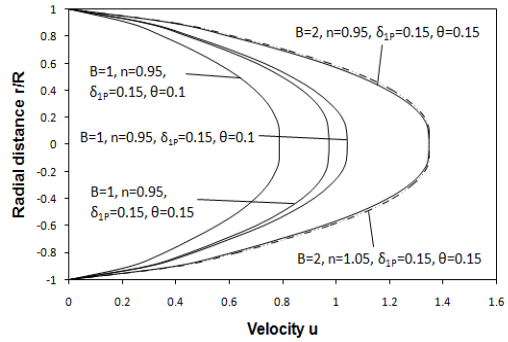

b. Two-phase H-B fluid model with β = 0.95.

Fig. 4. Velocity distribution for different values of *B*, *n*, δ_{1P} and θ with δ_{2P} = 0.1, α_H = 0.2 , ϕ = 0.2, ω = 1, z = 18.85.

3.4 Flow Rate

Fig. 5 shows the variation of flow rate of single-phase H-B fluid model with yield stress for different values of *B*, ϕ, α and δ_1 with $t = 296.47^o$, ω = 1, δ_2 = 0.1, n = 0.95, e = 0.5 and z = 18.85. It is seen that the flow rate decreases linearly with increasing yield stress θ. For a given set of values of the parameters α and δ_1, the flow rate increases considerably with the increase of the lead angle ϕ and it increases significantly with the increase of the body acceleration parameter *B*. It is also noted that the flow rate decreases slightly with the increase of the pulsatile Reynolds number ratio α and it decreases significantly with the increase of the maximum depth of the first stenosis when all the other parameters were kept as invariables. The Variation of flow rate of two-phase H-B fluid model with yield stress for different values of B, ϕ, α_H and e with ω = 1, $t = 296.47^\circ$, $\delta_{1P} = \delta_{2P} = 0.1$, n = 0.95, $\beta = 0.95$ and z = 18.85 is depicted in Fig. 6. It is observed that flow rate decreases linearly with the increase of the yield stress of the fluid. For a given set of values of the parameters B, e and ϕ, the flow rate decreases marginally with the increase of the pulsatile Reynolds number α_H of H-B fluid (fluid in the core region), whereas, the flow rate increases significantly with the increase of the body acceleration parameter B and it increases considerably with the increase of the lead angle ϕ and pressure gradient parameter e when all the other parameters were held fixed. From Figs. 5 and 6, one can observe that the flow rate of two-phase H-B fluid model is significantly higher than that of the single-phase H-B fluid model.

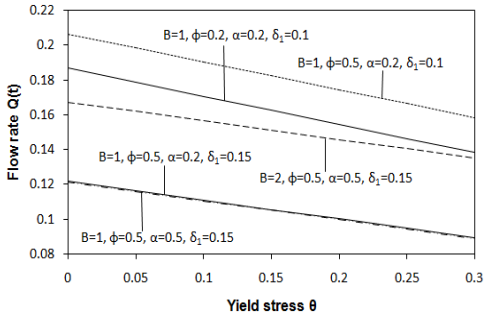

Fig.5. Variation of flow rate of single-phase H-B fluid model with yield stress for different values of *B*, ϕ, α and δ_1 with $t = 296.47^o$, ω = 1, δ_2 = 0.1, n = 0.95, e = 0.5 and z = 18.85.

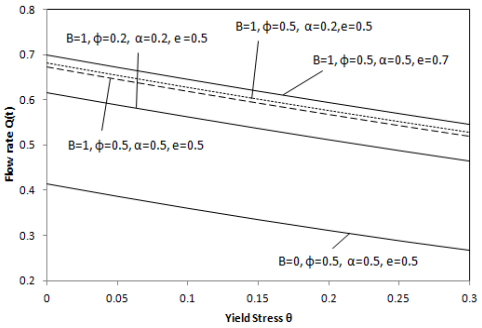

Fig. 6. Variation of flow rate of two-phase H-B fluid model with yield stress for different values of B, ϕ, α_H and e with ω = 1, n = 0.95, $t = 296.47^\circ$, $\delta_{1P} = \delta_{2P} = 0.1$, $\beta = 0.95$ and $z = 18.85$.

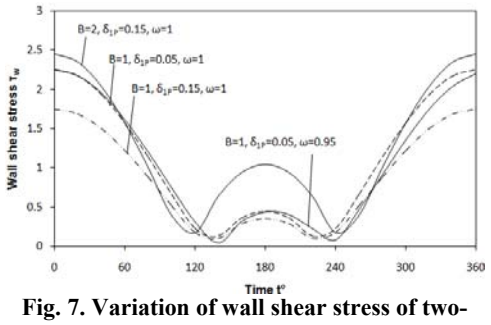

Fig. 7. Variation of wall shear stress of two-phase H-B fluid model in a time cycle for different values of B, δ_{1P}, α_H and θ with n = 0.95 , δ_{2P} = 0.1 , ϕ = 0, ω = 1, z = 18.85, β = 0.95 and e = 0.5.

3.5 Wall Shear Stress

The variation of wall shear stress of two-phase H-B fluid model in a time cycle for different values of B, δ_{1P} and ω with n = 0.95, δ_{2P} = 0.1, α_H = 0.2 , ϕ = 0, ω = 1, z = 18.85, β = 0.95 and e = 0.5 is exhibited in Fig. 7. One may observe that the wall shear stress decreases rapidly as time t increases from 0° to 140°and then it increases slowly with the increase of time t from 140° to 180° and then it decreases slowly with the increase of time t from 180° to 220° and thereafter it increases rapidly as time t increases from 220° to 360°. One may notice that when the maximum depth of the first stenosis in the peripheral layer region δ_{1P} increases, the wall shear stress decreases considerably in the time range 0° - 140° and 220° to 360° , decreases marginally in the time range 140° - 220°. It is also clear that the wall shear stress increases considerably with the increase of the body acceleration parameter B. When the parameters B and δ_{1P} held constant and the frequency parameter ω increases, the wall shear stress decreases very slightly in the time range 0° - 140°and 180° - 230° and then it increases very slightly in the time range 140° - 180°and 230° - 360°. Fig. 8 depicts the variation of wall shear stress of single-phase and two-phase H-B fluid models in a time cycle. It is noted that the wall shear stress of two-phase H-B fluid model is considerably lower than that of single-phase H-B fluid model and in the flow of both of the fluid models, the wall shear stress increases marginally with the increase of the pressure gradient parameter.

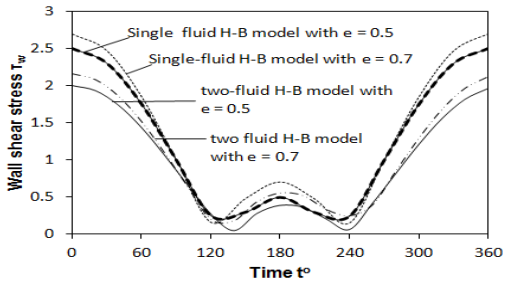

Fig. 8. Variation of wall shear stress with time for different fluid models with α_H = 0.2, ϕ = 0.2, e =0.5, β = 0.95, n = 0.95, δ_{1P} = 0.15, θ = 0.1, δ_{2P} = 0.1, ω = 1 and z = 18.85.

3.6 Longitudinal Impedance to Flow

The variation of longitudinal impedance to flow of single-fluid H-B model with pressure gradient parameter e for different values of B, ϕ and ω with θ = 0.1, n = 0.95, t = 296.47°, $\delta_1 = \delta_2 = 0.1$, z = 18.85 and $\alpha = 0.2$ is illustrated in Fig. 9. One can observe that the longitudinal impedance to flow decreases rapidly with the increase of pressure gradient parameter e from 0 to 1.5 and then it decreases very slowly when the pressure gradient parameter e increases from 1.5 to 6. It is noticed that the longitudinal impedance to flow decreases with the increase of the parameters B, ϕ and ω ; but the decrease in the longitudinal impedance to flow is marginal when lead angle ϕ increases, considerable when the body acceleration parameter B increases and significant when the frequency parameter ω increases. The variation of longitudinal impedance to flow of single-phase and two-fluid H-B models in a time cycle for different values of yield stress θ with t = 296.47°, B = 1, δ_{1P} = 0.15, δ_{2P} = 0.1, n = 0.95, e = 0.5, ω = 1, ϕ = 0.2, α_H = 0.2 and β = 0.95 is shown in Fig. 10. It is noted that the impedance to flow of two-phase H-B fluid model is marginally lower than that of single-phase H-B fluid model. It is clear that the impedance to flow increases significantly with the increase of the fluid's yield stress.

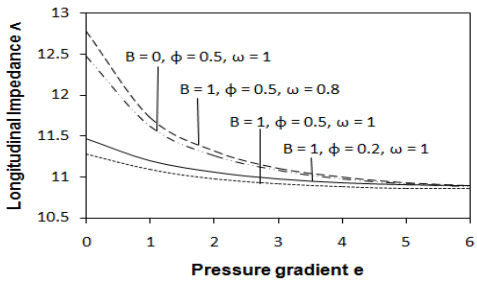

Fig. 9. Variation of longitudinal impedance to flow of single-phase H-B fluid model with pressure gradient for different values of B, ϕ and ω with θ = 0.1, n = 0.95, t = 296.47°, α = 0.2, δ_1 = δ_2 = 0.1 and z = 18.85.

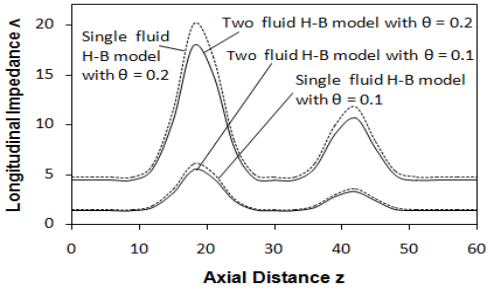

Fig. 10. Variation of longitudinal impedance to flow with axial distance for different fluid models when e = 0.5, α_H =0.5, n = 0.95, t = 296.47°, α = 0.2, ω = 1, δ_{1P} = 0.15, B = 1, δ_{2P} = 0.1 and β = 0.95.

3.7 Physiological Applications

To spell out some physiological applications of the

this study, the data (for different types of arteries, their corresponding radii, steady and pulsatile pressure gradient values) reported by Chaturani and Issac (1995) are reproduced in Table 1 and are used in our study to compute some important clinical measures of cardiovascular system. For arteries with different radii, the estimates of the mean velocity for two-phase and single-phase H-B fluid models for blood flow in narrow arteries with mild multiple-stenoses in the presence and absence of body acceleration with $t = 296.47^{\circ}$, $B = 1$, $\delta_{1P} = 0.15$, $\delta_{2P} = 0.1$, $n = 0.95$, $e = 0.5$, $\omega = 1$, $\phi = 0.2$, $\alpha = \alpha_H = 0.2$, and $\beta = 0.95$ are computed in Table 2. One can note that for both of the fluid models, the estimates of the mean velocity decreases significantly with the increase of radius of the artery except for the arteriole. It is also recorded that that the presence of body acceleration influences the mean velocity by increasing its magnitude significantly. It is found that the estimates of the mean velocity of the two-phase flow of blood are marginally higher than that of the single-phase flow of blood.

Table 1 Physiological data for different arteries.

Artery	Radius $\left(\text{x } 10^{-2} m\right)$	A_0 $\left(\text{x } 10 Kg\ m^{-2} s^{-1}\right)$	A_1 $\left(\text{x } 10 Kg\ m^{-2} s^{-1}\right)$
Aorta	1.0	7.3	1.46
Femoral	0.5	32.0	6.4
Carotid	0.4	50.0	10.0
Coronary	0.15	698.65	139.74
Arteriole	0.008	2000.0	400

Table 2 Estimates of mean velocity for two-phase and single-phase blood flow models for arteries with different radii.

Artery	Mean velocity with body acceleration $\left(\times 10^{-2} m/s\right)$		Mean velocity without body acceleration $\left(\times 10^{-2} m/s\right)$	
	Two-phase fluid model	Single-phase fluid model	Two-phase fluid model	Single-phase fluid model
Aorta	72.56	70.25	64.46	62.18
Femoral	80.23	76.45	70.61	68.72
Carotid	80.23	76.45	70.61	68.72
Coronary	155.68	150.42	133.74	129.4
Arteriole	1.3212	1.2732	1.1243	1.101

3.8 Discussion on the Results

The results obtained in this study bring out the following important observations.

- The presence of body acceleration enhances the velocity and flow rate and reduces the wall shear stress and longitudinal impedance to flow.
- The velocity and flow rate of the blood flow are considerably higher when is it modeled by two-phase H-B model compared to the corresponding flow quantities when it is modeled by single-phase H-B model.
- The wall shear stress and longitudinal impedance to flow of the blood flow are considerably lower when is it modeled by two-phase H-B model compared to the corresponding flow quantities when it is modeled by single-phase H-B model.

4. CONCLUSION

The present mathematical analysis spells out several useful and interesting rheological properties of blood when it flows through narrow arteries with mild axi-symmetric multiple-stenoses in the presence of periodic body acceleration, treating it as (i) single-phase H-B fluid model and (ii) two-phase H-B fluid model. Some major findings of this comparative analysis are listed below.

- The velocity decreases significantly with the increase of the yield stress and the reverse behavior is observed for longitudinal impedance to flow.
- The plug flow velocity, velocity distribution and flow rate are considerably higher for two-phase H-B fluid model than those of the single-phase H-B fluid model.
- The plug core radius, wall shear stress and longitudinal impedance to flow are marginally lower for two-phase H-B fluid model than those of the single-phase H-B fluid model.
- The estimates of the mean velocity are considerably higher for two-phase H-B fluid model than those of the single-phase H-B fluid.

From the results obtained in this investigation, it is observed that there is substantial difference between the flow quantities of single-fluid and two-phase H-B fluid models. Thus, it is expected that the use of two-phase H-B fluid model for blood flow in diseased artery may provide better results which may be used by the physicians to predict the effects of periodic body accelerations and different depths of stenoses in the artery on the physiologically important flow quantities. Also, one may hope that this analysis may provide some useful information to surgeons to take some crucial decisions regarding the treatment of patients, whether the vascular diseases can be treated with medicines or should the patient undergo a surgery. Hence, it is concluded that the present study may be considered as an improvement in the analysis of blood flow in narrow arteries with mild multiple-stenoses under periodic body accelerations.

REFERENCES

Ang, K.C. and J. Mazumdar (1995). Mathematical modeling of triple arterial stenosis, *Australian. Journal of Physical Engineering Science Medicine* 18, 89 – 94.

Chakravarthy, S. and P. K. Mandal (1996). A nonlinear two-dimensional model of blood flow in an overlapping arterial stenosis

subjected to body acceleration. *Math. Comp. Model*. 24, 43 – 58.

Chakravarthy, S. and P. K. Mandal (2000). Two-dimensional blood flow through tapered arteries under stenotic conditions. *Int. J. Non-Linear Mech*. 35, 779 – 793.

Chakravarty, S., S. Sarifuddin and P.K. Mandal (2004). Unsteady flow of a two-layer blood stream past a tapered flexible artery under stenotic conditions. *Computational Methods in Applied Mathematics* 4, 391-409.

Chaturani, P. and R. Ponnalagar Samy (1985). A study of non-Newtonian aspects of blood flow through stenosed arteries and its applications in arterial diseases. *Biorheology* 22, 521 – 531.

Chaturani, P. and V. Palanisami (1990). Casson fluid model of pulsatile flow of blood flow under periodic body acceleration, *Biorheology* 27, 619 – 630.

Chaturani P and S. A. W. Isaac (1995). Blood flow with body acceleration forces. *Int. J. Eng. Sci.* 33, 1807 – 1820.

El-Shahed, M. (2003). Pulsatile flow of blood through a stenosed porous medium under periodic body acceleration. *Appl. Math. Comput.* 138, 479 – 488.

El-Shehawey, E. F., E. M. E. Elbarbary, N. A. S. Afifi and M. El-Shahed (2000). MHD flow of an elastico-viscous fluid under periodic body acceleration. *Int. J. Math. & Math. Sci.* 23, 795 – 799.

Ikbal, M. A., S. Chakravarty, K. L. Kelvin Wong, J. Mazumdar and P. K. Mandal (2009). Unsteady response of non-Newtonian blood flow through a stenosed artery in magnetic field. *J. Comput. Appl. Math.* 230, 243-259.

Ismail, Z., I. Abdullah, N. Mustapha and N. Amin (2008). A power-law model of blood flow through a tapered overlapping stenosed artery. *Appl. Math. Comput.* 195, 669 – 680.

Liepsch, D., M. Singh and L. Martin (1992). Experimental analysis of the influence of stenotic geometry on steady flow. *Biorheology* 29, 419 – 431.

Liepsch, D. (2002). An introduction to bio-fluid mechanics, basic models and application. *J. Biomech.* 35, 415 - 435.

Liu, G. T., X. J. Wang, B. Q. Ai and L. G. Liu (2004). Numerical study of pulsating flow through a tapered artery with stenosis. *Chinese Journal of Physics* 42, 401 – 409.

Mandal, P. K., S. Chakravarthy, A. Mandal and N. Amin (2007). Effect of body acceleration on unsteady pulsatile flow of non-Newtonian fluid through a stenosed artery. *Applied Mathematics and Computation* 189, 766 – 779.

Misra, J. C. and B. Pal (1999). A mathematical model for the study of the pulsatile flow of blood under an externally imposed body acceleration. *Mathematical and Computer Modeling* 29, 89 – 106.

Misra, J. C. and S. K. Pandey (2002). Peristaltic transport of blood in small vessels: study of a mathematical model. *Computers and Mathematics with Applications* 43, 1183 – 1193.

Mustapha, N., S. Chakravarty, P. K. Mandal and N. Amin (2008). Unsteady response of blood flow through a couple of irregular arterial constrictions to body accelerations. *Journal of Mechanics and Medical Biology* 8, 395 – 420.

Nagarani, P. and G. Sarojamma (2008). Effect of body acceleration on pulsatile flow of Casson fluid through a mild stenosed artery. *Korea-Australia Rheology Journal* 20, 189 – 196.

Rogers, K. (2011). Blood: Physiology and Circulation, *Rosen Education Services,* ISBN-1615301216, 2011.

Sankar, D. S., J. Goh and A. I. M. Ismail (2010). FDM analysis for blood flow through stenosed tapered arteries. *Boundary Value Problems*, Article ID: 917067.

Sankar, D. S. (2010). Pulsatile flow of a two-fluid model for blood flow through arterial stenosis. *Mathematical Problems in Engineering*, Article

Sankar, D. S. and A. I. M. Ismail (2010). Effects of periodic body acceleration in blood flow through stenosed arteries – a theoretical model, *International Journal of Nonlinear Sciences and Numerical Simulations* 11, 243 – 257.

Sankar, D. S. (2010). Perturbation analysis for blood flow in stenosed arteries under body acceleration. *International Journal of Nonlinear Sciences and Numerical Simulations* 11, 631 – 653.

Sarojamma, G. and P. Nagarani (2002). Pulsatile flow of Casson fluid in a homogenous porous medium subject to external acceleration. *International Journal of Non-Linear Differential Equations.: Theory – Methods and Applications* 7, 50 – 64.

Siddiqui, S. U., N. K. Verma, S. Mishra and R. S. Gupta (2009). Mathematical modeling of pulsatile flow of Casson's fluid in arterial stenosis. *Applied Mathematics and Computation* 210, 1-10.

Srivastava, V .P. and M. Saxena (1994). Two-Layered model of Casson fluid flow through

stenotic blood vessels: Applications to the cardiovascular system. *Journal of Biomechanics* 27**,** 921 – 928.

Sud, V. K. and G. S. Sekhon (1985). Arterial flow under periodic body acceleration. *Bull. Math. Biol*. 47, 35 – 52.

Tu, C. and M. Deville (1996). Pulsatile flow of non-Newtonian fluids through arterial stenosis. *Journal of Biomechanics* 29, 899–908.

Usha, R. and K. Prema (1999). Pulsatile flow of particle-fluid suspension model of blood under periodic body acceleration. *ZAMP* 50, 175 – 192.

Appendix A

Solving Eqs. (9) and (11) with the help of the boundary conditions (12) and (13) and Eqs. (14) – (19), one can obtain the following expressions for τ_{P1}, τ_{H1}, u_{H1} and u_{P1} (Sankar and Ismail, 2010).

$$\tau_{P1} = -\left[g(t)R\right]^n DR^2\left[\left(n/\left(2(n+1)\right)\right)\left(q^2/R\right) -\left((n-1)/2\right)\left(q^2/R\right)^2 -\left(n/\left(2(n+1)\right)\right)\left(q^2/R\right)^{n+2}\right] \quad \text{(A1)}$$

$$\tau_{H1} = -\left[g(z)R\right]^n DR^2 \times\left[\left(n/\left((n+1)(n+3)\right)\right)\left\{\left((n+3)/2\right)(r/R)-(r/R)^{n+2}\right\} -\left((n-1)/(n+2)\right)\left(q^2/R\right)\left\{\left((n+2)/2\right)(r/R)-(r/R)^{n+1}\right\} -\left(3\left(n^2+2n-2\right)/2(n+2)(n+3)\right)\left(q^2/R\right)^{n+3}(R/r)\right] \quad \text{(A2)}$$

$$u_{H1} = -2n\left[g(t)R\right]^{2n-1} DR^3\left[n/\left(2(n+1)^2(n+3)\right)\right. \times\left\{(n+2)-(n+3)(r/R)^{n+1}+(r/R)^{2n+2}\right\} +\left((n-1)/\left(2(n+1)(n+2)(n+3)(2n+1)\right)\right)\left(q^2/R\right) \times\left\{(n+2)(n+3)(2n+1)\left[(r/R)^n+(r/R)^{n+1}\right]\right. -2\left[\left(2n^3+9n^2+11n+3\right)+\left(2n^2+6n+3\right)(r/R)^{2n+1}\right] +\frac{(n-1)^2}{2n(n+2)}\left(\frac{q^2}{R}\right)^2\left\{(n+1)-(n+2)\left[\frac{r}{R}\right]^n+\left[\frac{r}{R}\right]^{2n}\right\} +\frac{3\left(n^2+2n-2\right)}{2(n-1)(n+2)(n+3)}\left(\frac{q^2}{R}\right)^{n+3}\left\{\left(\frac{r}{R}\right)^{n-1}-1\right\}\Bigg\} +\frac{3\left(n^2+2n-2\right)(n-1)}{2(n-2)(n+2)\ (n+3)}\left(\frac{q^2}{R}\right)^{n+4}\left\{1-\left[\frac{r}{R}\right]^{n-2}\right\}\Bigg] \quad \text{(A3)}$$

where $D = (1/g)(dg/dt)$.

Appendix B

From Eq. (6) and the expressions for velocity, the expression for the volumetric flow rate $Q(z,t)$ is obtained as below.

$$Q(z,t) = 4\left[\left(\int_0^{R_{P0}} r\,u_{P0}\,dr + \int_{R_{P0}}^{R} r\,u_{H0}\,dr\right) +\alpha_H^2\left(\int_0^{R_{P0}} r\,u_{P1}\,dr + \int_{R_{P0}}^{R} r\,u_{H1}\,dr\right)\right]$$
$$= \left(\left[g(t)R\right]^n R^3/\left((n+2)(n+3)\right)\right) \times\left[\left\{(n+2)-n(n+3)\left(q^2/R\right)+\left(n^2+2n-2\right)\left(q^2/R\right)^{n+3}\right\} -\alpha_H^2\left[g(t)R\right]^{n-1}\left(nDR^2/4\right) \times\left\{n-\left(2n(n-1)\left(4n^2+12n+5\right)/\left((2n+1)(2n+3)\right)\right)\left(q^2/R\right) +\left(n(n-1)^2(n+3)/(n+1)\right)\left(q^2/R\right)^2 +\left(\left(n^3-2n^2-11n+6\right)/(n+1)\right)\left(q^2/R\right)^{n+3} -\left((n-1)\left(n^3-2n^2-11n+6\right)/n\right)\left(q^2/R\right)^{n+4} -\left(\left(4n^5+14n^4-8n^3-45n^2-3n+18\right)/n(n+1)(2n+3)\right)\left(q^2/R\right)^{2n+4}\right\}\Bigg] \quad \text{(B1)}$$

Appendix C

Eqs (39) - (46) form a system of partial differential equations which can be solved for the unknowns $u_{0H}, u_{1H}, \tau_{0H}, \tau_{1H}, u_{0N}$, u_{1N}, τ_{0N} and τ_{1N} with the help of boundary conditions (47) - (51) and the expressions obtained for these quantities are obtained as below.

$$\tau_{P0} = g(t)R_{P0}; \quad \tau_{H0} = g(t)r; \quad \tau_{N0} = g(t)r;$$
$$u_{N0} = g(t)R^2\left[1-(r/R)^2\right] \quad \text{(C1)}$$

$$u_{H0} = \left[g(t)R\right]R\left\{1-(R_1/R)^2+2[g(t)R_1]^n R_1 \times\left[\left(1/(n+1)\right)\left\{1-(r/R_1)^{n+1}\right\}-\left(q^2/R_1\right)\left\{1-(r/R_1)^n\right\}\right] \quad \text{(C2)}$$

$$u_{P0} = \left[g(t)R\right]R\left\{1-(R_1/R)^2+2[g(t)R_1]^n R_1 \times\left[\left(1/(n+1)\right)\left\{1-(R_{0P}/R_1)^{n+1}\right\}-\left(q^2/R_1\right)\left\{1-(R_{0P}/R_1)^n\right\}\right] \quad \text{(C3)}$$

$$\tau_{P1} = -\frac{1}{4}[g(t)R]DR^2\left(\frac{q^2}{R}\right)\left\{1-\left(\frac{R_1}{R}\right)^2\right\}-[g(t)R_1]^n DR_1^2 \times\left[\frac{n}{2(n+1)}\left(\frac{q^2}{R_1}\right)-\frac{(n-1)}{2}\left(\frac{q^2}{R_1}\right)^2-\frac{n}{2(n+1)}\left(\frac{q^2}{R_1}\right)^{n+2}\right] \quad \text{(C4)}$$

$$\tau_{H1} = -(1/4)[g(t)R]DR^2(r/R)\left\{1-(R_1/R)^2\right\} -[g(t)R_1]^n DR_1^2\left[\frac{n}{(n+1)(n+3)}\left\{\left(\frac{n+3}{2}\right)\left(\frac{r}{R_1}\right)-\left(\frac{r}{R_1}\right)^{n+2}\right\} -\frac{(n-1)}{(n+2)}\left(\frac{q^2}{R_1}\right)\left\{\left(\frac{n+2}{2}\right)\left(\frac{r}{R_1}\right)-\left(\frac{r}{R_1}\right)^{n+1}\right\} -\left(3(n^2+2n-2)/(2(n+2)(n+3))\right)\left(q^2/R_1\right)^{n+3}(R_1/r)\right] \quad \text{(C5)}$$

$$\tau_{N1} = -[g(t)R]DRR_1\left[\frac{1}{4}\left(\frac{r}{R_1}\right)-\frac{1}{8}\left(\frac{R_1}{R}\right)^2\left(\frac{R_1}{r}\right)-\frac{1}{8}\left(\frac{R_1}{R}\right)^2\left(\frac{r}{R_1}\right)^3\right] -[g(t)R_1]^n DR_1^2\left[\frac{n}{2(n+3)}\left(\frac{R_1}{r}\right)-\frac{n(n-1)}{2(n+2)}\left(\frac{q^2}{R_1}\right)\left(\frac{R_1}{r}\right)\right.$$

$$-\left(3(n^2+2n-2)/\left(2(n+2)(n+3)\right)\right)\left(q^2/R_1\right)^{n+3}\left(R_1/r\right)\Bigg] \quad \text{(C6)}$$

$$u_{N1}=-2\left[g(t)R\right]DR^2R_1\Bigg[\left(1/8\right)\left(R/R_1\right)\left\{1-\left(r/R\right)^2\right\}$$

$$-\left(1/8\right)\left(R_1/R\right)^3\log\left(R/r\right)-\left(1/32\right)\left(R/R_1\right)\left\{1-\left(r/R\right)^4\right\}\Bigg]$$

$$-2[g(t)R_1]^n DR_1^3\log\left(R/r\right)$$

$$\times\left[\frac{n}{2(n+3)}-\frac{n(n-1)}{2(n+2)}\left(\frac{q^2}{R_1}\right)-\frac{3(n^2+2n-2)}{2(n+2)(n+3)}\left(\frac{q^2}{R_1}\right)^{n+3}\right] \quad \text{(C7)}$$

$$u_{H1}=-2[g(t)R]DR^2R_1$$

$$\times\left[\frac{3}{32}\left(\frac{R}{R_1}\right)-\frac{1}{8}\left(\frac{R_1}{R}\right)+\frac{1}{32}\left(\frac{R_1}{R}\right)^3+\frac{1}{8}\left(\frac{R_1}{R}\right)^3\log\left(\frac{R_1}{R}\right)\right]$$

$$+2[g(t)R_1]^n DR_1^3\log\left(R_1/R\right)$$

$$\times\left[\frac{n}{2(n+3)}-\frac{n(n-1)}{2(n+2)}\left(\frac{q^2}{R_1}\right)-\frac{3(n^2+2n-2)}{2(n+2)(n+3)}\left(\frac{q^2}{R_1}\right)^{n+3}\right]$$

$$-n[g(t)R_1]^n DR_1R^2\left\{1-\left(R_1/R\right)^2\right\}$$

$$\times\left[\frac{1}{2(n+1)}\left\{1-\left(\frac{r}{R_1}\right)^{n+1}\right\}-\frac{(n-1)}{2n}\left(\frac{q^2}{R_1}\right)\left\{1-\left(\frac{r}{R_1}\right)^n\right\}\right]$$

$$-2n[g(t)R_1]^{2n-1}DR_1^3\Bigg[\left(n/2\left(n+1\right)^2\right)\left\{1-\left(r/R_1\right)^{n+1}\right\}$$

$$-\left((n-1)/2\left(n+1\right)\right)\left(q^2/R_1\right)\left\{1-\left(r/R_1\right)^n\right\}$$

$$-\left(n/\left(2(n+1)^2(n+3)\right)\right)\left\{1-\left(r/R_1\right)^{2n+2}\right\}$$

$$+\frac{(n-1)(2n^2+6n+3)}{(n+1)(n+2)(n+3)(2n+1)}\left(\frac{q^2}{R_1}\right)\left\{1-\left(\frac{r}{R_1}\right)^{2n+1}\right\}$$

$$-\frac{(n-1)}{2(n+1)}\left(\frac{q^2}{R_1}\right)\left\{1-\left(\frac{r}{R_1}\right)^{n+1}\right\}+\frac{(n-1)^2}{2n}\left(\frac{q^2}{R_1}\right)^2$$

$$\times\left\{1-\left(\frac{r}{R_1}\right)^n\right\}-\frac{(n-1)^2}{2n(n+2)}\left(\frac{q^2}{R_1}\right)^2\left\{1-\left(\frac{r}{R_1}\right)^{2n}\right\}$$

$$-\frac{3(n^2+2n-2)}{2(n-1)(n+2)(n+3)}\left(\frac{q^2}{R_1}\right)^{n+3}\left\{1-\left(\frac{r}{R_1}\right)^{n-1}\right\}$$

$$+\frac{3(n-1)(n^2+2n-2)}{2(n-2)(n+2)(n+3)}\left(\frac{q^2}{R_1}\right)^{n+4}\left\{1-\left(\frac{r}{R_1}\right)^{n-2}\right\}\Bigg] \quad \text{(C8)}$$

where $r\big|_{\tau_{P0}=\theta}=R_{P0}=\theta/g\left(t\right)=q^2$, $q^2=\left(\theta/g(t)\right)$, $g\left(t\right)=\left(1+e\cos t\right)+\mathrm{B}\cos\left(\omega\tau+\phi\right)$, $B=\left(1/g\right)\left(dg/dt\right)$. One can refer Sankar (2010c) for details of obtaining the above expressions.

Appendix D

Using the expression obtained for velocity distribution in Eq. (36), the expression for the volumetric flow rate $Q\left(z,t\right)$ can be obtained as given below.

$$Q=4\Bigg[\int_0^{R_{0P}}\left(u_{P0}+\alpha_H^2u_{P1}\right)r\,dr$$

$$+\int_{R_{0P}}^{R_1}\left(u_{H0}+\alpha_H^2u_{H1}\right)r\,dr+\int_{R_1}^{R}\left(u_{N0}+\alpha_N^2u_{N1}\right)r\,dr\Bigg]$$

$$=4\left[g(t)R\right]R^3\left\{1-\left(R_1/R\right)^2\right\}\Bigg[\left(q^2/R_1\right)^2+\left(1/4\right)\left\{1-\left(R_1/R\right)^2\right\}\Bigg]$$

$$+\left(4[g\left(t\right)R_1]^n\,R_1^3/\left(\left(n+2\right)\left(n+3\right)\right)\right)$$

$$\times\left[(n+2)-n(n+3)\left(q^2/R_1\right)+(n^2+2n-2)\left(q^2/R_1\right)^{n+3}\right]$$

$$+4\alpha_H^2\Bigg[-[g(t)R]^n DR^2{R_1}^3$$

$$\times\left\{\frac{3}{32}\left(\frac{R}{R_1}\right)-\frac{1}{8}\left(\frac{R_1}{R}\right)+\frac{1}{32}\left(\frac{R_1}{R}\right)^3+\frac{1}{8}\left(\frac{R_1}{R}\right)^3\log\left(\frac{R_1}{R}\right)\right\}$$

$$+[g(t)R_1]^n DR_1^5\log\left(R_1/R\right)$$

$$\times\left\{\frac{n}{2(n+3)}-\frac{n(n-1)}{2(n+1)}\left(\frac{q^2}{R_1}\right)-\frac{3(n^2+2n-2)}{2(n+2)(n+3)}\left(\frac{q^2}{R_1}\right)^{n+3}\right\}$$

$$-n\left[g(t)R_1\right]^n DR^2R_1^3\left\{1-\left(R_1/R\right)^2\right\}\left\{\left(1/4(n+3)\right)\right.$$

$$\left.-\left((n-1)/4(n+2)\right)\left(q^2/R_1\right)+\left(\left(n^2+n-5\right)/4(n+2)(n+3)\right)\left(q^2/R_1\right)^{n+3}\right\}$$

$$-n[g(t)R_1]^{2n-1}DR_1^5\left\{\left(n/\left(2(n+2)(n+3)\right)\right)\right.$$

$$\left.-\left(n(n-1)(4n^2+12n+5)/\left((n+2)(n+3)(2n+1)(2n+3)\right)\right)\left(q^2/R_1\right)\right.$$

$$\left.+\left(n(n-1)^2/\left(2(n+1)(n+2)\right)\right)\left(q^2/R_1\right)^2\right.$$

$$+4\alpha_N^2\Big[-[g(t)R]DR^4R_1\left\{\left(1/24\right)\left(R/R_1\right)-\left(3/32\right)\left(R_1/R\right)\right.$$

$$\left.+\left(5/96\right)\left(R_1/R\right)^5-\left(1/8\right)\left(R_1/R\right)^3\log\left(R_1\right)\left\{1-\left(R_1/R\right)^2\right\}\right\}$$

$$-[g(t)R_1]^n DR^2R_1^3\left\{1-\left(R_1/R\right)^2\right\}(1+2\log R_1)$$

$$\left\{\frac{n}{4(n+3)}-\frac{n(n-1)}{4(n+2)}\left(\frac{q^2}{R_1}\right)+\frac{3(n^2+2n-2)}{4(n+2)(n+3)}\left(\frac{q^2}{R_1}\right)^{n+3}\right\}\Bigg] \quad \text{(D1)}$$